IN VITRO AND *IN VIVO* CHARACTERISATION OF ISOLATES OF *CRYPTOCOCCUS NEOFORMANS* CAUSING MENINGITIS IN HIV INFECTED AND UNINFECTED PATIENTS IN VIETNAM

Thanh Tuan Lam[1], Dena Toffaletti[2], Jennifer Tenor[2], Charles Giamberardino[2], Gregory D. Sempowski[3], Yohannes Asfaw[4], Trieu Hai Phan[1], Anh Van Duong[1], Trinh Mai Nguyen[1], Lan Phu Huong Nguyen [5],Chau Thi Hong Tran [1], Philip M. Ashton[1], Justin Beardsley[1],Chau Van Vinh Nguyen [6], Guy E. Thwaites[1], Stephen Baker[1], John R. Perfect[2], Jeremy N. Day[1,5]

[1]Oxford University Clinical Research Unit, Hospital for Tropical Diseases, Ho Chi Minh City, Vietnam

[2]Division of Infectious Diseases, Department of Medicine and Department of Molecular Genetics and Microbiology, Duke University, North Carolina, USA

[3]Duke Human Vaccine Institute and Regional Biocontainment Laboratory, Duke University, North Carolina, USA

[4]Division of Laboratory Animal Resources, Duke University, North Carolina, USA

[5]Nuffield Department of Clinical Medicine, Centre for Tropical Medicine and Global Health, University of Oxford, Oxford, UK

[6]Hospital for Tropical Diseases, Ho Chi Minh City, Vietnam

Corresponding author: Jeremy N Day: jday@oucru.org

Running title: Characterizing *Cryptococcus neoformans* from HIV infected and uninfected patients

Keywords

Cryptococcal meningitis*, Cryptococcus neoformans,* MLST*,* immunocompetent*,* HIV-uninfected, HIV, A/J mice, ST5, phenotype

Abstract

Most cryptococcal meningitis cases occur in immunocompromised individuals and are caused by *Cryptococcus neoformans* var.*grubii.* We previously reported cryptococcal meningitis in Vietnam arising atypically in HIV-uninfected, apparently immunocompetent patients, caused by a single amplified fragment length polymorphism (AFLP) cluster of *C. neoformans* (VNI-γ). This variant was less common in HIV-infected individuals. It is unclear why this lineage is associated with HIV-uninfected, apparently immunocompetent patients. To better delineate the phenotypic characteristics of *C. neoformans* VNI-γ in comparison with other *C. neoformans* lineages we selected 30 representative isolates and compared their genotype-specific *in vitro* pathogenic potential and *in vivo* virulence, and ability to induce inflammatory response in the A/J mouse model. All isolates were genotyped using multi-locus sequence typing. All previously AFLP-defined VNI-γ isolates were identified as sequence type (ST) 5. Compared with non-ST5 strains, ST5 isolates had significantly increased variability in cell and capsule size (p<0.001). ST5 and non-ST5 strains exhibited similar characteristics in relation to previously defined virulence factors including melanization, growth at 37°C, and growth in cerebrospinal fluid. However, A/J

mice infected with ST5 isolates had significantly longer survival and lower fungal burdens at day 7 and death compared with non-ST5 isolates. ST5 isolates induced significantly greater initial inflammatory responses than non-ST5 strains, measured by TNF-α concentrations ($p<0.001$). Despite being generally less virulent in the mouse model, we hypothesize that the significant within strain variation seen in ST5 isolates in the tested phenotypes may represent an evolutionary advantage enabling adaptation to novel niches including apparently immunocompetent human hosts.

Introduction

Cryptococcal meningitis (CM) is a life-threatening fungal infection. The largest burden of CM occurs in immunocompromised individuals, including those with HIV infection, malignancy, organ failure, autoimmune disease, and receiving immunomodulatory therapy (1, 2). Globally, CM is estimated to result in 120,000 to 240,000 deaths per year (3). Most cases of CM are associated with two species: *Cryptococcus neoformans* and *Cryptococcus gattii* (2, 4). *C. neoformans* is more commonly associated with CM in immunocompromised patients and incorporates two varietal forms: *C. neoformans* var.*grubii* and *C. neoformans* var. *neoformans*. *C. neoformans* var.*grubii* is isolated globally while *C. neoformans* var. *neoformans* is more commonly isolated from patients in Europe (5, 6). The burden of CM is highest in sub-Saharan Africa and South/Southeast Asia where there are more people living with HIV/AIDS. In these tropical and subtropical regions, *C. gattii* CM is relatively uncommon in HIV-infected patients, usually accounting for only 1-2% of cryptococcosis in HIV-infected individuals, although higher rates have been reported from Botswana and Malawi (up to 30% of all CM cases) (7, 8). It is

widely acknowledged that *C. gattii* primarily causes disease in immunocompetent patients while *C. neoformans* is associated with disease in immunocompromised patients(9, 10).

Where CM due to *C. neoformans* var.*grubii* occurs in HIV-uninfected individuals, reports most often describe patients with an increased disease susceptibility due to some other underlying immunosuppressive condition (11–13). However, in Australasia and the USA no clear underlying immune deficit is identified in approximately 20% of CM cases in HIV-uninfected individuals (14–19). In Vietnam, disease in HIV-uninfected patients accounts for approximately 10% of all CM cases admitted to our referral hospital in Ho Chi Minh City (HCMC) (20). We have previously reported that the majority of HIV-uninfected patients had no identified cause of immunosuppression, and that >80% of HIV-uninfected CM patients were infected by yeasts belonging to a single amplified fragment length polymorphism (AFLP)-defined cluster of *C. neoformans*, which we had named VNI-γ (19, 20). Our clinical observation has been replicated in China where over 70% of CM cases from apparently immunocompetent individuals were infected with *C. neoformans* (17). The yeasts isolated from these immunocompetent patients in China were closely related to each other, and belonged to a single multi-locus sequence type (MLST), sequence type (ST)5 (17). Similarly, this ST accounted for more than 80% of non-HIV-associated cases of CM in South Korea, although some patients from this group had other underlying, potentially immunosuppressive conditions. (21). The association between a particular ST/genotype and host immune phenotype could be explained by a lineage-specific increase in pathogenic potential or microbial fitness, a currently unidentified host immune deficit, or a combination of these factors.

In order to explore the hypothesis that VNI-γ strains have increased pathogenic potential, we compared their virulence phenotypes in a range of in vitro experiments with non-VNI-γ strains. Additionally, we exploited a mouse model of cryptococcosis to compare the relative *in vivo* virulence and the differential immune responses of Vietnamese clinical isolates from CM patients with and without HIV.

Material and methods

C. neoformans organisms and culture conditions

The yeasts used in this study were clinical isolates from the cerebrospinal fluid (CSF) of patients enrolled in a randomized controlled trial of antifungal therapy in HIV-infected patients, and a prospective, descriptive study of HIV-uninfected patients with central nervous system (CNS) infections (20, 22). All studies were approved by the Institutional Review Board of the Hospital for Tropical Diseases, Ho Chi Minh City, and the Oxford Tropical Ethics Committee or Liverpool School of Tropical Medicine UK. All yeasts were archived at -80°C in Microbank beads (Pro-Lab Diagnostics, UK). We randomly selected 30 isolates for characterization (15 from HIV-infected patients and 15 from HIV-uninfected patients), from which eight representative isolates were randomly selected for assessment of *in vivo* virulence in A/J mice. For each isolate, a single colony was selected from the initial archive and purified for all subsequent experiments. For each experiment, a single purified *C. neoformans* colony was inoculated into 5ml of Yeast Peptone Dextrose (YPD) broth and incubated overnight at 30°C with agitation. Cells were harvested and washed three times with phosphate-buffered saline (PBS). Inoculum

quantification was performed using a Cellometer X2 (Nexelom Biosciences, USA). The cryptococcal mating type was determined by polymerase chain reaction amplification of the MAT locus as previously described (23). The characteristics of the selected yeasts and the clinical data from the corresponding patients are shown in Table 1.

DNA extraction and Multi-locus Sequence Typing (MLST) determination

All isolates have been previously genotyped using amplified fragment length polymorphism (AFLP) (19). Total genomic DNA was extracted using the Masterpure Yeast DNA kit (Epicentre Biotechnologies, Madison, WI, USA) according to the manufacturer's instructions after growth on Sabouraud agar. Seven MLST loci (CAP59, GPD1, IGS1, LAC1, PLB1, SOD1, and URA5) were amplified and sequenced following the procedures of the International Society for Human and Animal Mycology (ISHAM) MLST consensus typing scheme for *C. neoformans* (http://mlst.mycologylab.org)(24). Sequencing was performed using BigDye v3.1 Chemistry (Applied Biosystems, CA, USA) on an ABI 3130 Genetic Analyzer (Applied Biosystems, CA, USA). Both forward and reverse amplicons of each locus were sequenced. Consensus sequences were manually edited using ContigExpress and aligned in AlignX , implemented in VectorNTI Suite 7.0 (InforMax, USA) (25). A single Allele Type (AT) number was assigned to each of the seven loci using the ISHAM database (http://mlst.mycologylab.org)(24), resulting in a seven-number allelic profile for each isolate. The allelic profiles defined the corresponding STs.

Ex vivo CSF growth, melanin production, and temperature–dependent growth

We measured growth of the various *C. neoformans* strains at different temperatures and in *ex vivo* human CSF following previously described procedures with modifications for quantitative assessment (26). To assess fungal growth at selected temperatures, inocula were adjusted to 10^6 cells/ml, serially diluted, and inoculated in duplicate onto YPD agar plates in 5ul aliquots and incubated at 30°C or 37°C for 48 hours. After 48 hours, colony forming units (CFU) were counted. For the *ex vivo* CSF experiment, CSF supernatant from three random de-identified HIV-infected patients enrolled into an antifungal therapy trial was pooled, filtered, and stored at -80°C until use (22). Growth was assessed by adding 10ul of 10^6 cells/ml into 90ul of the pooled CSF and incubating at 37°C in 5%CO_2; CSF was serially diluted and inoculated onto YPD agar at days 1 and 3 post-inoculation. All experiments were repeated in triplicate. *C. neoformans* H99 was included as a control in all experiments; data were standardized by expressing the growth results as a ratio of the CFU of the clinical yeast isolate to the CFU of H99. Melanin production was assessed by plating a drop of cell suspension (10^6/mL) onto L-DOPA agar (1g/L L-asparagine , 1g/L glucose, 3g/L KH_2PO_4, 250mg/L $MgSO_4.7H_2O$, 1mg/L Thiamine HCl, 5µg/L Biotin, 100mg/L L-DOPA, 20g/L Bacto Agar)(27, 28). Plates were incubated in the dark at 30°C or 37°C for 3 days. Differences in melanization were compared visually with a melanotic control strain.

145 ***Capsule and cell size measurement***

146 To measure the capsule thickness of yeasts grown *in vitro*, all isolates were sub-cultured onto
147 DMEM media (Dulbeco Modified Eagle Medium powder with 4.5g/L glucose L-glutamine,
148 sodium pyruvate (without $NaHCO_3$),; $NaHCO_3$ 250mM (Merck); NaMOPS 1M; Neomycin
149 200mg/ml, Cefotaxime 100 mg/ml; (29) and incubated at 37°C in 5% CO_2 until single colonies
150 were visible. Unless otherwise specified, all reagents were purchased from Sigma-Alrich. India-
151 ink-stained smears were prepared on a microscope slide and visualized at 100X magnification
152 using light microscopy (CX41, Olympus, Japan). Images were captured using a DP71 Camera
153 system with DP Controller software (Olympus, Japan) and processed using ImageJ
154 (rsb.info.nih.gov/ij/). Capsular thickness was calculated by subtracting the cell body diameter
155 (D_{CD}, no capsule) from whole cell diameter (D_{WC}, including capsule). At least 30 individual cells
156 were measured for each isolate.

157

158 ***Mouse infection model of cryptococcosis***

159 All mouse infections were conducted as previously described (30) and were performed
160 according to Duke University's Institutional Animal Care and Use Committee guidelines and
161 approvals.

162 The virulence of each individual strain was assessed by measuring survival rate and fungal
163 burden in tissue from two independent experiments. Six week old female A/J mice were lightly
164 sedated with isoflurane and infected intranasally with the selected cryptococcal strain by
165 dropping 25ul of yeast suspension containing $5x10^4$ cells into the nares (31, 32). Animals were

166 monitored daily. Mice showing signs of distress or losing more than 15% body weight were
167 euthanized by CO_2 inhalation. Survival assays were performed using 10 mice per strain.

168 To measure fungal burden in the mice, five animals were infected with each clinical isolate and
169 euthanized by CO_2 inhalation either on day 7 or day 14 post-infection, or when the animal
170 showed signs of distress or had lost >15% of initial body weight. Fungal burden was assessed by
171 excising the left superior lobe of the lung and homogenizing the tissue by bead beating. Tissue
172 homogenates were serially diluted and plated onto YPD agar supplemented with 100mg/ml
173 ampicillin. The plates were incubated at 30°C for 48 hours and the number of *C. neoformans*
174 colony forming units (CFU) recorded. Fungal burdens were expressed as CFU per gram of tissue
175 (CFU/g). At the same time points (7 and 14 days post-infection), the right superior lobe of the
176 lung from each mouse was excised and immersed in 10% formalin (replaced with 70% Ethanol
177 after 24 hours) for histopathology. Fixed specimens were stored at 4°C until processing. After
178 paraffin embedding, sliced sections were stained using the Period Acid-Schiff method (PAS).
179 Histopathological examination was performed by an independent pathologist blinded to the
180 infecting strain. The resulting tissue damage was scored from 0 (no changes) to 10 (severe
181 changes), corresponding to the severity of pathology in 4 different categories: necrosis,
182 hemorrhage, edema and inflammation as per the Duke Veterinary Diagnostic Laboratory
183 (Division of Laboratory Animal Resources).

184

185 To assess the severity of the inflammatory responses the middle lobe from the right lung of
186 each infected mouse was excised and homogenized by bead beating in 1ml sterile PBS/Protease
187 inhibitor. 500ul of lung homogenate was used for cytokine profiling. Cytokines representing T-

helper type 1 (Th1) (IL-12p70, TNF-α, IFN-γ), T-helper type 17 (IL-17) and T-helper type 2 (Th2) (IL-4, IL-5, IL-10) responses were measured using a customized Bio-Plex Pro™ Mouse Cytokine Th1/Th2 Assay kit (Biorad, USA) with the BioPlex 200 platform according to the manufacturer's guidelines. Data were retrieved using BioPlex Manager software. The upper and lower limits of quantification (ULOQ and LLOQ) were based on a standard curve. All values falling below the LLOQ were replaced with the midpoint between zero and the LLOQ. Data were standardized by lung weight and presented as pg of cytokines per gram lung tissue (pg/g).

Statistical analysis

GraphPad Prism version 5.04 for Windows (GraphPad Software, San Diego California USA; www.graphpad.com) was used for data visualization and statistical analyses of fungal loads, cytokine profiling, capsular/cell size, and survival proportions. Mann-Whitney U-test was used for comparing fungal load and cytokine concentrations. Kaplan-Meier survival curves, and the log-rank test were used for survival analysis. Capsule/cell size was analyzed in GraphPad Prism 5.04 for Windows (GraphPad Software, San Diego California USA; www.graphpad.com) and compared using Welch's t-test. The Fligner-Killeen test of variance homogeneity for analyzing variation in capsule/cell size and Fisher's exact test were performed using R software, version 3.2.4 (http://www.r-project.org). One way ANOVA with a post hoc multiple comparison test (Dunnett or Bonferroni) integrated in Graphpad was used to compare cytokine concentrations between individual isolates.

The study was approved by the scientific committee of the Hospital for Tropical Diseases, Ho Chi Minh City, Vietnam. All animal experiments were performed according to Duke University's Institutional Animal Care and Use Committee guidelines and approvals.

Results

Multi-locus Sequence Typing of Vietnamese C. neoformans isolates

All 30 isolates selected for characterization in the study were confirmed to be *C. neoformans* serotype A, mating type α (Aα). MLST of the 30 isolates identified four different STs: ST4 (12/30), ST5 (15/30), ST6 (2/30), and ST306 (1/30). All 15 of the previous described AFLP VNI-γ isolates were ST5, while the 15 AFLP VNI-δ (non- VNI-γ) isolates comprised three different STs (ST4, ST6, and ST306). None of the HIV-uninfected patients with an ST5 infection had any other known or apparent underlying diseases. The two HIV-uninfected patients with an identified underlying disease (lupus and gastric cancer) were infected with an ST4 and a ST306 *C. neoformans*, respectively.

In vitro phenotyping of Vietnamese C. neoformans isolates

Upon microscopic examination we observed that the ST5 *C. neoformans* isolates developed significantly thicker capsule during *in vitro* culture than non-ST5 isolates (mean 2.64 µm [95%CI: 2.49 - 2.79µm] versus mean 2.01µm [95%CI: 1.94 - 2.07µm], respectively, $p<0.0001$, Welch's t-test; also see Table 2). Individual ST5 *C. neoformans* cells were also significantly larger in size than cells from the non-ST5 strains (cell diameter excluding the capsule 11.38µm [95%CI: 10.96

- 11.79µm] versus mean 9.69µm [95%CI: 9.52 - 9.87µm], respectively, $p<0.0001$, Welch's t-test; also see Table 2). In fact, a high degree of variation in capsule size and cell diameter was detected in yeast isolates belonging to ST5 (Figure 1); a Fligner-Killeen test for homogeneity of variance confirmed this variation to be significantly greater for ST5 than non-ST5 isolates ($p<0.0001$) for both capsule size and cell diameter). Strains of both lineages tended to appear less melanized at 37°C, in comparison to the control strain, H99 (see Supplementary Figure S1). However, there were no genotype-specific differences in either growth at 30°C ($p=0.10$, Welch's t-test; mean CFU/ml ratio to H99: 0.98[95%CI:0.74 to 1.22] for ST5 vs 1.01[95%CI:0.87 to 1.15] for non ST5) or 37°C ($p=0.23$, Welch's t-test; mean CFU/ml ratio to H99: 1.2[95%CI:0.98 to 1.42] for ST5 vs 1.11[95%CI:0.85 to 1.37] for non ST5) , or *ex vivo* survival in CSF after one day exposure ($p=0.72$, Welch's t-test; mean CFU/ml ratio to H99: 11.72[95%CI:2.07 to 21.36] for ST5 vs 5.84[95%CI:1.37 to 10.31] for non ST5 at day 1; or *ex vivo* survival in CSF for three days exposure: $p=0.77$, Welch's t-test; mean CFU/ml ratio to H99: 1.36[95%CI:0.67 to 2.06] for ST5 vs 3.23[95%CI:1.31 to 5.16] for non ST5 at day 3) (see Supplementary Figures S2 and S3). Representative phenotyping data are shown in Supplementary Figures S4 and S5.

Mouse infection model of cryptococcosis with Vietnamese C. neoformans isolates

Animals were challenged individually with five randomly-chosen different ST5 strains (BK147, BK44, BMD700, BMD1338 and BMD1646) and three non-ST5 strains (BMD1415, BK80 (both ST4) and BMD1367 (ST306)). Infections with the ST5 strains were associated with significantly longer survival time than infection with the` non-ST5 strains ($p<0.0001$, log-rank test, Figure 2). However, there was significant variability in the effect of individual yeast strains of the same

lineage on survival time (Supplementary Figure S6). Notably, two ST5 isolates strains (BK147 and BMD1646) appeared to be substantially attenuated in comparison to the other ST5 yeast strains with mice infected with these yeasts surviving up to day 40 post infection. However, the differences in survival times between mice infected with ST5 and non-ST5 strains remained significant when data from these two isolates were removed from the comparative analysis (p=0.003, log-rank test, data not shown). Of the eight strains selected for infecting mice, the two most virulent were BMD1415 (ST4), and BMD1338 (ST5); infection with these isolates resulted in 100% mortality by days 17 and 18, respectively (median survival 15 and 17 days, respectively). BMD1338 was significantly less virulent than BMD1415 (p=0.0015, log-rank test). No significant difference in virulence was detected between BMD1338 and BMD1367, the second most virulent non-ST5 strain. Although it was not as virulent as isolates BMD700 and BMD1338, the ST5 isolate BK44 also resulted in 100% mortality by day 25.

All strains successfully established lung infection and disseminated to the brain of the mice as early as day 7. Consistent with the survival data, the non-ST5 strains established a higher fungal burden in the lung than the ST5 organisms at all time points (p=0.0002, p<0.0001, and p<0.0001 at day 7, day 14, and at the point of 15% weight loss, respectively, Mann-Whitney U-test) (Figure 3). Moreover, these data were not driven by the two severely attenuated isolates (BK147 and BMD1646) as the fungal loads associated with ST5 infections remained low even when these two isolates were excluded from the analysis. The majority of mice infected with BMD1646 (ST5) and BK147 (ST5) became sterile and therefore lung fungal burdens in these animals were minimal up to day 14. On the other hand, despite these differences in fungal

burden in the lung, there were no ST5/non-ST5 specific differences in fungal burden in the brain up to day 14. However, brain fungal burdens in non-ST5 infections were significantly higher than the brain fungal burdens in ST5 infections at the point of 15% weight loss (mean logCFU.g^{-1} (95%CI); 4.5 (3.9-4.7) and 2.9 (2.2-3.6) for non-ST5 and ST5 respectively, *p*=0.01, Mann-Whitney U-test). Again, as seen with yeast cell size, significantly more intra-genotypic variation in mice fungal burden was observed amongst the ST5 strains than amongst non-ST5 strains (*p*<0.001, Fligner-Killeen test).

Inflammatory responses induced during a mouse infection model of cryptococcosis with C. neoformans from HIV-uninfected patients

We next measured the concentration of cytokines from lung homogenates of A/J mice infected with the various strains at days 7 and day 14 post-infection. Cytokine concentrations at these time points are shown in Figure 4, according to the genotype of the infecting organism. At day 7, ST5 strain infections were associated with significantly higher concentrations of TNF-α in the lung than non-ST5 strain infections (*p*=0.01, Mann-Whitney U-test; also see Table 4). Furthermore, among ST5 strain infections at day 7, TNF-α concentrations were highest for the two specific strains that appeared to be most attenuated in the mouse survival model (BK147 and BMD1646), and lowest in BMD1338, the most virulent ST5 isolate in the mouse model. By day 14, mean TNF-α concentration associated with the ST5 strains had declined from 3933.71 pg/g to 2802.36 pg/g. Other Th-1 cytokines including IL-12, IL-17 and IFN-γ also decreased in ST5-infected mice between day 7 and day 14 (p<0.001, p<0.01 and p=0.02, Mann-Whitney U-test, respectively).

This contrasted with non-ST5 strain infections, in which mean TNF-α levels increased from 3256.25 pg/g to 6378.76 pg/g (p=0.0003 and p=0.0235, Mann-Whitney U-test, respectively; also see Table 4) between days 7 and 14. However, the high concentration of TNF-α seen in non-ST5 strain infections at day 14 was driven by a single isolate - BMD1415; TNF-α concentrations in the lung in mice infected with this isolate were significantly higher than for infections with any other ST5 or non-ST5 isolate (p<0.05, Mann-Whitney U-test). There were no statistically significant differences in TNF-α concentration at day 14 when data from infections due to this isolate were excluded from the analysis. The same BMD1415-driven pattern also occurred when comparing IFN-γ and IL-17 concentrations at day 14. The concentrations of these two cytokines in BMD1415-infected mice appeared significantly higher than in mice infected with any other isolates (p<0.05, Mann-Whitney U-test; see Supplementary Figure S7). However, IL-12 concentrations fell in non-ST5 strain infected mice, including BMD1415, between day 7 and 14 (4 fold decrease, p<0.0001, Mann-Whitney U-test) (Figure 5).

We measured the TNF-α/IL-10 ratio as a proxy marker of the relationship between a Th-1 and a Th-2 response (33). From day 7 to day 14 post-infection, the TNF-α: IL-10 ratio decreased almost 1.28 fold in mice infected with ST5 isolates while those infected with non-ST5 strains exhibited a TNF-α: IL-10 ratio increase of 1.25 fold. However, when BMD1415 (ST4) was excluded from the analysis the TNF-α/IL-10 ratio in mice infected with non-ST5 strains decreased by a factor of 0.67. By day 14 we detected elevated concentrations of IL-17 and IFN-γ in non-ST5 infected mice (5-fold and 17-fold increments, respectively (Table 4), but not in ST5 infected mice. Again, this effect was largely associated with BMD1415, since the concentrations

of IL-17 and IFN-γ induced by this isolate at day 14 were significantly higher than for all others ($p<0.05$, one way ANOVA test; also see Supplementary Figure S7).

Histological examination of infected lung tissue revealed evidence of inflammation, hemorrhage, edema and necrosis in most cases. These changes were generally greater by day 14 in comparison to day 7. There were no clear differences in histological scores between sequence types, other than strain BMB1646 (ST5) which had only mild inflammation with no necrosis or haemorrhage seen (Figure 6, also see Supplementary Figure S8). Though we could not quantitatively assess and compare genotype-specific capsule size *in vivo,* ST5 yeasts appeared extensively encapsulated in the lung sections, especially at day 14 (Figure 6). This observation agreed with the previous finding that ST5 isolates have increased *in vitro* capsular induction.

Discussion

Although *C. gattii* disease is well recognized in immunocompetent hosts worldwide [30], most cases in apparently immunocompetent patients in Asia, including Vietnam, are due to *C. neoformans* var.*grubii* [15,20,31,32]. We previously reported that 84% of *C. neoformans* infections in HIV-uninfected patients in Vietnam are caused by a single AFLP-defined cluster (VNI-γ); here we confirm these strains as MLST ST5, consistent with studies reported from China, Japan and Korea [17,21,33,34]. It is unlikely that the high prevalence of ST5 infection observed in HIV- uninfected patients is simply explained by significantly greater prevalence of this lineage in the environment (and subsequent greater exposure) since ST5 accounts for only

35% of cases of disease in HIV- infected patients [19] within the same geographical area. Furthermore, in the same locales ST5 is not more prevalent in any particular HIV- associated sub-group such as intravenous drug users [19].

The high prevalence of ST5 strain infection in HIV-uninfected patients could be explained either by the strains being intrinsically more virulent, or lineage–specific unidentified host immune defects or exposures. In this study we investigated the first hypothesis by comparing previously identified virulence-associated phenotypes (capsule size, *ex vivo* growth in CSF, cell wall melanization and growth at human body temperature) as well as *in vivo* virulence and immune responses in the mouse model by lineage [35–43]. Strains from all STs were able to grow in human CSF and at 37°C - essential characteristics for human infections. However, we could not identify ST-specific differences of growth under these conditions, suggesting that the ability to establish disease in HIV-uninfected/immunocompetent patients is not driven by simple adaptations to high temperature or growth in human CSF.

On the other hand, we found ST5 cells to be both significantly larger than non-ST5 cells and to have thicker capsules in vitro, which might impact pathogenic potential [44–47]. The capsule of *C. neoformans* plays important roles in pathogenesis, from interfering with phagocytosis by host macrophages to modulating the host immune response [48–52]. Previously, it has been shown that *in vitro*-induced capsular enlargement confers greater virulence in CBA/J mice [53–55], and that variations in capsule size also correlate with pathogenic potential including overcoming *in vivo* phagocytosis by host macrophages, leading to uncontrolled fungal growth and host cell death [50,53,55]. *Ex vivo* capsule size has also been associated with higher intracranial pressure, slower clearance of yeasts and paucity of inflammation in humans(34).

Our study demonstrates that while ST5 isolates have significantly higher capacity for *in vitro* capsule enlargement, this phenotype did not translate into increased virulence in the mouse model. Mice infected with ST5 isolates not only had better survival but also lower tissue fungal burdens than those infected with non-ST5 strains, contrary to recent human data which supports morphological changes being associated with more severe pathology in the human host (e.g *ex vivo* capsule size and capsular shedding has been associated with increased intracranial pressure in CM patients with HIV)(34).

There are several possible explanations for the lower virulence of ST5 in mice we observed. First, virulence in mice is variable depending on mouse breed and may not accurately reflect the immunological heterogeneity of the human population [56]. Second, yeasts with different pathogenic potentials, associated with their isolation from different sources (i.e. clinical versus environmental, immunocompromised vs immunocompetent patients) may have the same or paradoxical pathogenic potential in experimental animal models. For instance, *C. gattii* is often associated with infection in immunocompetent patients and therefore is considered more virulent (or fit) in the human host than *C. neoformans*. However, it has been shown that the *C. gattii* strain R265, responsible for the on-going Vancouver outbreak, has similar virulence in both C57BL/6 and A/J mice to the *C. neoformans* H99 strain, which is derived from a patient on chemotherapy with Hodgkin's disease [57]. Furthermore, the same study reported it was impossible to distinguish the virulence of strain R272, a Vancouver outbreak *C. gattii* VGIIb strain, from WM276, an environmental isolate from Australia, with either murine model [57]. Third, the A/J mouse strain is not immunologically intact and thus may be an imperfect model of infection for immunocompetent hosts [58,59]. Rather, it may be a better model of disease in

immunosuppressed patients, as the mice are highly susceptible to cryptococcal disease, and the patterns of cytokine expression in mice with disseminated cryptococcosis are similar to those seen in HIV-infected patients with CM [1,60]. Our results suggest that additional models to the mouse may be needed to explain the complex interaction between *C. neoformans* and the human host, particularly when the host is apparently immunocompetent.

In cryptococcal infection in mice, a Th1 type immune response, defined by the TNF-α/IL-10 ratio, is considered to be protective, while a Th2 response is associated with poor outcomes [61,62]. We did not detect genotypic-driven changes in TNF-α/IL-10 ratios over time, although higher TNF-α concentrations were induced by ST5 strains at day 7 suggesting this genotype elicited a more intense initial inflammatory response. This finding could be explained by the increased capsular size of ST5 organisms - previous studies have suggested that capsule components, or cryptococcal cells themselves, have a dose-dependent ability to stimulate TNF-α production by various immune effector cells [13,63–67]. We found that ST5 organisms induced stronger inflammatory response in mice even though the ST5 fungal burden was around 5 times lower than that of non-ST5 organisms 7 days post-infection, suggesting that TNF-α production may be driven by capsular components rather than cell number. Previously, it has been suggested that *C. gattii* is able to cause disease in apparently immunocompetent patients because it induces a less severe inflammatory response than other cryptococci [57]. Data generated from our murine infection experiments do not support a less severe inflammatory response being the mechanism underlying the ability of ST5 organisms to cause disease in the immunocompetent.

In vivo controlled infection studies in mice commonly define pathogenicity as the microbe's capability to cause disease in a susceptible host, whereas virulence corresponds to the severity of the ensuing pathology [68]. Using the same infective dose for all strains we failed to demonstrate that ST5 strains had greater virulence than non-ST5 organisms. The difference we observe in prevalence of different lineages in immunocompetent and immunosuppressed human patients may alternatively represent a specific difference in the ability of the organisms to colonize the host and establish infection; we were not able to assess this with our experimental systems. Spores are presumed to be the main infectious propagule for *Cryptococcus* spp, although desiccated yeast cells have also been proposed [69]. Capsule biosynthesis genes are required for both efficient sexual development and spore formation and dispersal [70]. Given the higher rate of capsular enlargement and higher variation in capsule size in ST5 strains, it is possible that capsule biosynthesis genes are more active in ST5 yeasts, resulting in qualitative differences in their spores that confer higher infectivity when interacting with immunocompetent hosts. Moreover, the higher rates of variability that we see in this and other virulence phenotypes (for example, growth at 37C, see supplementary information) within ST5 strains in this study hint that higher phenotypic variability in ST5 may be an adopted strategy that facilitates the exploitation of novel niches. This strategy could have resulted in a phenotype which allowed the successful colonization of one or more novel environmental nich(es), and as a bystander-effect, allowed the exploitation of infrequent specific human immune deficits. Thus, our cohort of ST5 yeast isolates displayed two notable phenotypes. First, in general they appeared to be less virulent in a murine model than the other sequence types, as demonstrated by reduced fungal burdens in tissue, induction of greater early

immunological responses and prolonged mouse survival. Second, ST5 strains had larger capsules and cell sizes than the other genotypes, and notably greater variability between individual strains for this phenotype.

Our data lead us to three main conclusions. First, clinical isolates, which have by their nature already undergone selection within the human host, can possess wide variability in the expression of virulence phenotypes within a single lineage. Secondly, the use of host risk factors and immune phenotype to derive an understanding of the factors that drive the pathogenicity of *Cryptococcus* may be more complex than anticipated. Associations may be difficult to make due to the relevance of the particular *in vitro* phenotypes, animal models used, within strain heterogeneity, and population substructure. Moreover, there may be significant heterogeneity in the immune response of apparently immunocompetent patients which selects particular sub-cohorts of isolates of the same lineage. Thirdly, the categorization of strains into specific clades with limited genetic information such as MLST may lack precision to understand the relative fitness of specific strains in the human host. It is likely that whole genome sequencing will provide better mapping of the relationships between strains and virulence. Lastly, we tested a relatively small number of strains, and may have lacked power to detect relevant differences that are present at the wider population level.

Conclusions

In this study, we demonstrated genotype-specific differences in *in vitro* and *in vivo* virulence phenotypes between *C. neoformans* var.*grubii* strains isolated from host with different immune status. There was also significant variation among strains isolated from apparently immunocompetent patients in specific *in vitro* and *in vivo* phenotypes tested. This higher rate

of phenotypic variation may represent an evolutionary strategy for *C. neoformans* var.*grubii* to take advantage of novel niches and contribute to their ability to infect apparently immunocompetent hosts, despite generally being less virulent in a mammalian animal model. Furthering the understanding of the pathogenesis of cryptococcal meningitis will require investigation of large numbers of strains with associated robust clinical information, and the development of high throughput laboratory phenotypic studies that have clinical relevance in humans.

Acknowledgements

JND is a Wellcome Trust Intermediate Fellow (WTWT097147MA). SB is a Sir Henry Dale Fellow, jointly funded by the Wellcome Trust and the Royal Society (100087/Z/12/Z). Multiplex cytokine profiling was performed in the Immunology Unit of the Duke Regional Biocontainment Laboratory, which received partial support for construction from the US National Institutes of Health, National Institute of Allergy and Infectious Diseases (UC6-AI058607).

References

1. Heitman J, Kozel TR, Kwon-Chung KJ, Perfect JR, Casadevall A. 2011. Cryptococcus: From human pathogen to model yeast. ASM Press, Washington DC.

2. Casadevall A, Perfect JR. 1998. *Cryptococcus neoformans*. ASM Press, Washington DC.

3. Rajasingham R, Smith RM, Park BJ, Jarvis JN, Govender NP, Chiller TM, Denning DW, Loyse A, Boulware DR. 2017. Global burden of disease of HIV-associated cryptococcal meningitis: an updated analysis. Lancet Infect Dis.

4. Kwon-Chung KJ, Varma A. 2006. Do major species concepts support one, two or more species within *Cryptococcus neoformans*? FEMS Yeast Res 6:574–87.

5. Bennett JE, Kwon-Chung KJ, Howard DH. 1977. Epidemiologic differences among serotypes of *Cryptococcus neoformans*. Am J Epidemiol 105:582–6.

6. Dromer F, Mathoulin S, Dupont B, Laporte a. 1996. Epidemiology of cryptococcosis in France: a 9-year survey (1985-1993). French Cryptococcosis Study Group. Clin Infect Dis 23:82–90.

7. Bogaerts J, Rouvroy D, Taelman H, Kagame A, Aziz MA, Swinne D, Verhaegen J. 1999. AIDS-associated cryptococcal meningitis in Rwanda (1983-1992): epidemiologic and diagnostic features. J Infect 39:32–7.

8. Litvintseva AP, Thakur R, Reller LB, Mitchell TG. 2005. Prevalence of clinical isolates of *Cryptococcus gattii* serotype C among patients with AIDS in Sub-Saharan Africa. J Infect Dis 192:888–892.

9. Cogliati M. 2013. Global Molecular Epidemiology of *Cryptococcus neoformans* and *Cryptococcus gattii*: An Atlas of the Molecular Types. Scientifica (Cairo) vol. 2013:23 pages.

10. Speed B, Dunt D. 1995. Clinical and host differences between infections with the two varieties of *Cryptococcus neoformans*. Clin Infect Dis 21:28–34; discussion 35–6.

11. Rozenbaum R, Gonçalves AJR. 1994. Clinical epidemiological study of 171 cases of cryptococcosis. Clin Infect Dis 18:369–380.

12. Shih CC, Chen YC, Chang SC, Luh KT, Hsieh WC. 2000. Cryptococcal meningitis in non-HIV-infected patients. QJM 93:245–251.

13. Mitchell DH, Sorrell TC, Allworth AM, Heath CH, McGregor AR, Papanaoum K, Richards MJ, Gottlieb T. 1995. Cryptococcal disease of the CNS in immunocompetent hosts: Influence of cryptococcal variety on clinical manifestations and outcome. Clin Infect Dis 20:611–616.

14. Lui G, Lee N, Ip M, Choi KW, Tso YK, Lam E, Chau S, Lai R, Cockram CS. 2006. Cryptococcosis in apparently immunocompetent patients. QJM 99:143–51.

15. Pappas PG, Perfect JR, Cloud G a, Larsen R a, Pankey G a, Lancaster DJ, Henderson H, Kauffman C a, Haas DW, Saccente M, Hamill RJ, Holloway MS, Warren RM, Dismukes WE. 2001. Cryptococcosis in human immunodeficiency virus-negative patients in the era of effective azole therapy. Clin Infect Dis 33:690–9.

16. Kiertiburanakul S, Wirojtananugoon S, Pracharktam R, Sungkanuparph S. 2006. Cryptococcosis in human immunodeficiency virus-negative patients. Int J Infect Dis 10:72–8.

17. Chen J, Varma A, Diaz M. 2008. *Cryptococcus neoformans* strains and infection in apparently immunocompetent patients, China. Emerg Infect Dis 14.

18. Chen S, Sorrell T, Nimmo G, Speed B, Currie B, Ellis D, Marriott D, Pfeiffer T, Parr D, Byth K. 2000. Epidemiology and host- and variety-dependent characteristics of infection due to *Cryptococcus neoformans* in Australia and New Zealand. Australasian Cryptococcal Study Group. Clin Infect Dis 31:499–508.

19. Day JN, Hoang TN, Duong A V, Hong CTT, Diep PT, Campbell JI, Sieu TPM, Hien TT, Bui T, Boni MF, Lalloo DG, Carter D, Baker S, Farrar JJ. 2011. Most cases of cryptococcal meningitis in HIV-uninfected patients in Vietnam are due to a distinct Amplified Fragment Length Polymorphism-defined cluster of *Cryptococcus neoformans* var. *grubii* VN1. J Clin Microbiol 49:658–664.

20. Chau TT, Mai NH, Phu NH, Nghia HD, Chuong L V, Sinh DX, Duong V a, Diep PT, Campbell JI, Baker S, Hien TT, Lalloo DG, Farrar JJ, Day JN. 2010. A prospective descriptive study of cryptococcal meningitis in HIV uninfected patients in Vietnam - high prevalence of *Cryptococcus neoformans* var. *grubii* in the absence of underlying disease. BMC Infect Dis 10:199.

21. Choi YH, Ngamskulrungroj P, Varma A, Sionov E, Hwang M, Carriconde F, Meyer W, Litvintseva AP, Gyo W, Shin JH, Kim E-CC, Lee KW, Choi TY, Seon Y, Hwang SM, Carriconde F, Meyer W, Litvintseva AP, Lee WG, Shin JH, Kim E-CC, Lee KW, Choi TY, Lee YS, Kwon-Chung KJ. 2010. Prevalence of the VNIc genotype of *Cryptococcus neoformans* in non-HIV associated cryptococcosis in the Republic of Korea. FEMS Yeast Res 10:769–778.

22. Day JN, Chau TTH, Wolbers M, Mai PP, Dung NT, Mai NH, Phu NH, Nghia HD, Phong ND, Thai CQ, Thai LH, Chuong L V, Sinh DX, Duong VA, Hoang TN, Diep PT, Campbell JI, Sieu TPM, Baker SG, Chau NV V, Hien TT, Lalloo DG, Farrar JJ. 2013. Combination antifungal therapy for cryptococcal meningitis. N Engl J Med 368:1291–302.

23. Chaturvedi S, Rodeghier B, Fan J, McClelland CM, Wickes BL, Chaturvedi V. 2000. Direct PCR of *Cryptococcus neoformans* MATalpha and MATa pheromones to determine mating

529 type, ploidy, and variety: a tool for epidemiological and molecular pathogenesis studies. J
530 Clin Microbiol 38:2007–9.

531 24. Meyer W, Aanensen DM, Boekhout T, Cogliati M, Diaz MR, Esposto MC, Fisher M,
532 Gilgado F, Hagen F, Kaocharoen S, Litvintseva AP, Mitchell TG, Simwami SP, Trilles L,
533 Viviani MA, Kwon-Chung J. 2009. Consensus multi-locus sequence typing scheme for
534 *Cryptococcus neoformans* and *Cryptococcus gattii*. Med Mycol 47:561–570.

535 25. Lu G, Moriyama EN. 2004. Vector NTI, a balanced all-in-one sequence analysis suite. Brief
536 Bioinform 5:378–388.

537 26. Lee A, Toffaletti DL, Tenor J, Soderblom EJ, Thompson JW, Moseley MA, Price M, Perfect
538 JR. 2010. Survival defects of *Cryptococcus neoformans* mutants exposed to human
539 cerebrospinal fluid result in attenuated virulence in an experimental model of meningitis.
540 Infect Immun 78:4213–25.

541 27. Salas SD, Bennett JE, Kwon-Chung KJ, Perfect JR, Williamson PR. 1996. Effect of the
542 laccase gene CNLAC1, on virulence of *Cryptococcus neoformans*. J Exp Med 184:377–386.

543 28. Eisenman HC, Mues M, Weber SE, Frases S, Chaskes S, Gerfen G, Casadevall A. 2007.
544 *Cryptococcus neoformans* laccase catalyses melanin synthesis from both D- and L-DOPA.
545 Microbiology 153:3954–3962.

546 29. Zaragoza O, Casadevall A. 2004. Experimental modulation of capsule size in *Cryptococcus*
547 *neoformans*. Biol Proced Online 6:10–15.

548 30. Hu G, Cheng PY, Sham A, Perfect JR, Kronstad JW. 2008. Metabolic adaptation in
549 *Cryptococcus neoformans* during early murine pulmonary infection. Mol Microbiol

69:1456–1475.

31. Wormley FL, Cox GM, Perfect JR. 2005. Evaluation of host immune responses to pulmonary cryptococcosis using a temperature-sensitive *C. neoformans* calcineurin A mutant strain. Microb Pathog 38:113–23.

32. Cox GM, Mukherjee J, Cole GT, Casadevall A, Perfect JR. 2000. Urease as a virulence factor in experimental cryptococcosis. Infect Immun 68:443–8.

33. Levitz SM, Tabuni A, Nong SH, Golenbock DT. 1996. Effects of interleukin-10 on human peripheral blood mononuclear cell responses to *Cryptococcus neoformans*, Candida albicans, and lipopolysaccharide. Infect Immun 64:945–51.

34. Robertson EJ, Najjuka G, Rolfes M a, Akampurira A, Jain N, Anantharanjit J, von Hohenberg M, Tassieri M, Carlsson A, Meya DB, Harrison TS, Fries BC, Boulware DR, Bicanic T. 2014. *Cryptococcus neoformans* ex vivo capsule size is associated with intracranial pressure and host immune response in HIV-associated cryptococcal meningitis. J Infect Dis 209:74–82.

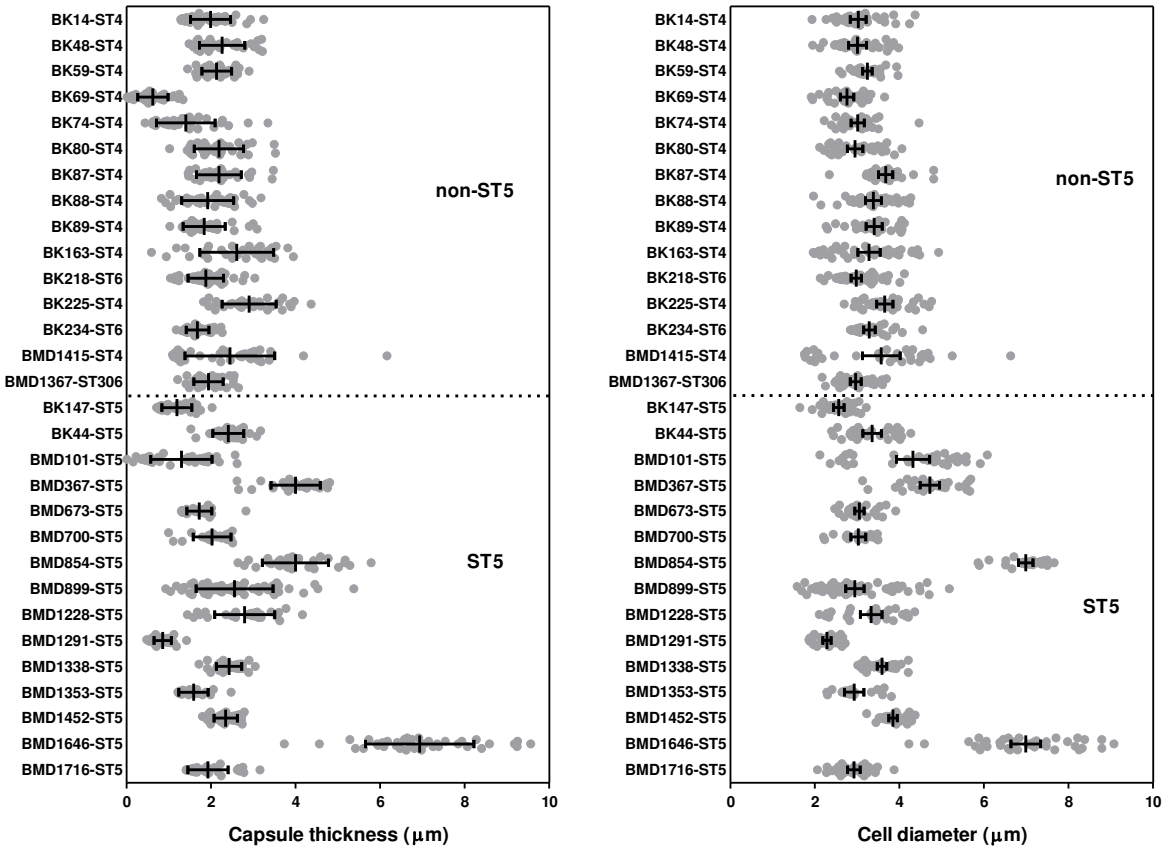

FIGURE 1: *In vitro* induced capsule thickness and cell diameter of individual *Cryptococcus neoformans* strains from Vietnam: Cells were grown on DMEM medium/5% CO_2 and visually assessed by India ink staining. Images were taken for single cells measurement using ImageJ software. Capsule thickness is obtained by subtracting cell body diameter from total cell diameter. AFLP-VNI-γ/MLST-ST5 strains expressed higher degree of variation in both capsule size and cell diameter *in vitro*. Scattered plot represents single cells from an individual strain. Data for individual strains are presented as mean with error bars denoting standard deviation.

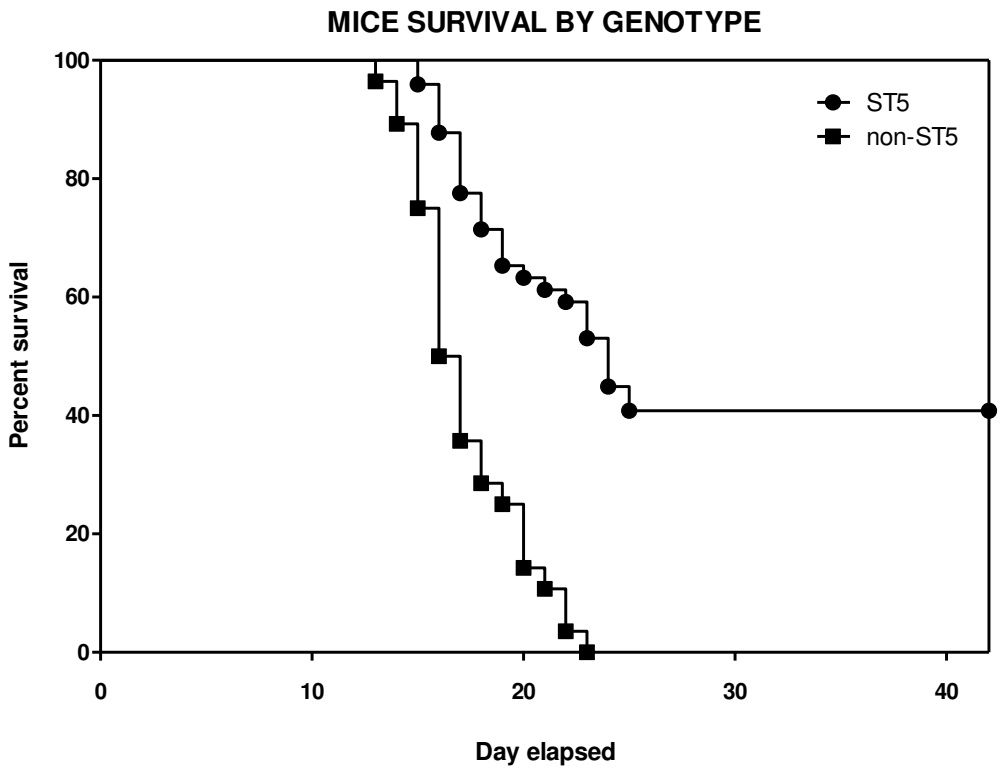

FIGURE 2: Kaplan-Meier survival curves for mice infected with either VNI-γ or VNI-δ *Cryptococcus neoformans* strains. 10 mice were infected per strain **ST5** N = 5, **non-ST5** N = 3). Mice were monitored daily until the point of more than 15% weight loss or visible suffering and were then sacrificed by CO_2 inhalation. Mice infected with ST5 strains had statistically significantly longer survival times than those infected with non-ST5 strains ($P<0.0001$, Mantel-Cox log rank test).

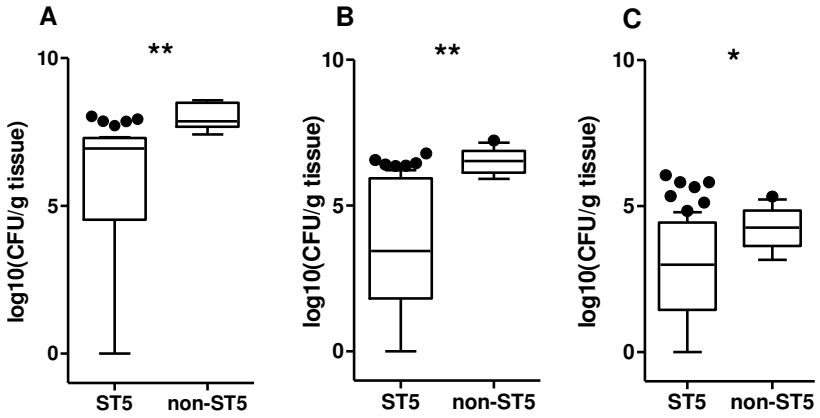

FIGURE 3: Fungal burden in lung tissue at day 14 (A), lung fungal burden at point of impending death (B) and brain fungal burden at point of impending death (C) according to infecting genotype. 5 mice were infected per strain **(ST5** N = 5, **non-ST5** N = 3). Mice were monitored daily until there was > 15% weight loss or visible suffering and were then sacrificed by CO_2 inhalation. Non-ST5 fungal burden appeared higher than that of ST5 in both lung and brain tissue at all time points (Mann-Whitney test, **: P<0.0001, *: P<0.05). The horizontal line within the box indicates the median; boundaries of the box indicate the 25th and 75th percentile and the whiskers indicate the highest and lowest values of the results; outliers are denoted as black dots.

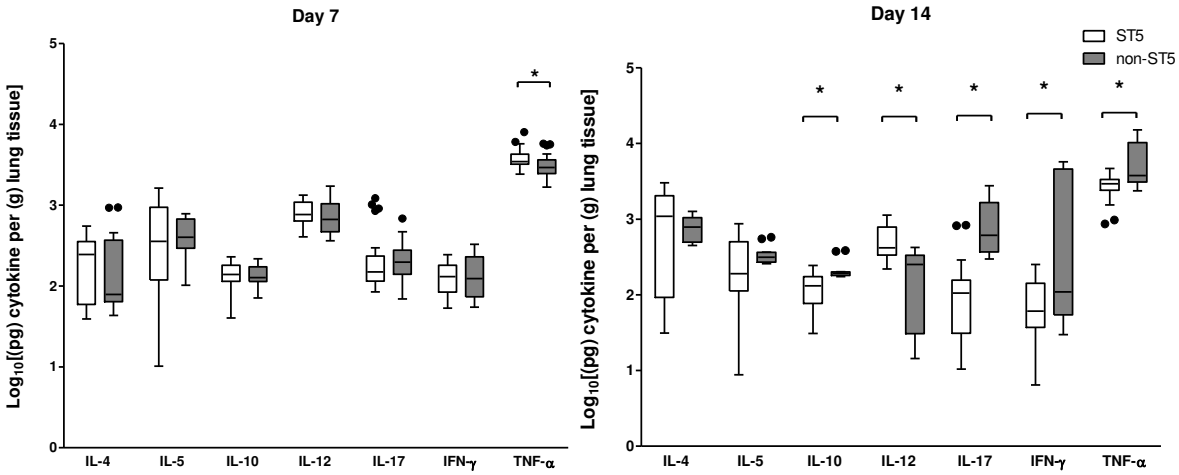

FIGURE 4: Genotype-specific cytokines concentrations from lung homogenate of A/J mice at 7 and 14 days post infection with 5x10^4 *C. neoformans* cells/mouse. Box and whisker plots compare levels of each cytokine between each genotype at day 7 and day 14 post-infection. The horizontal line within the box indicates the median; boundaries of the box indicate the 25th and 75th percentile and the whiskers indicate the highest and lowest values of the results; outliers are denoted as black dots. Data are standardized as picogram of cytokine per gram lung tissue. Asterisks show statistical significance by Mann-Whitney test.

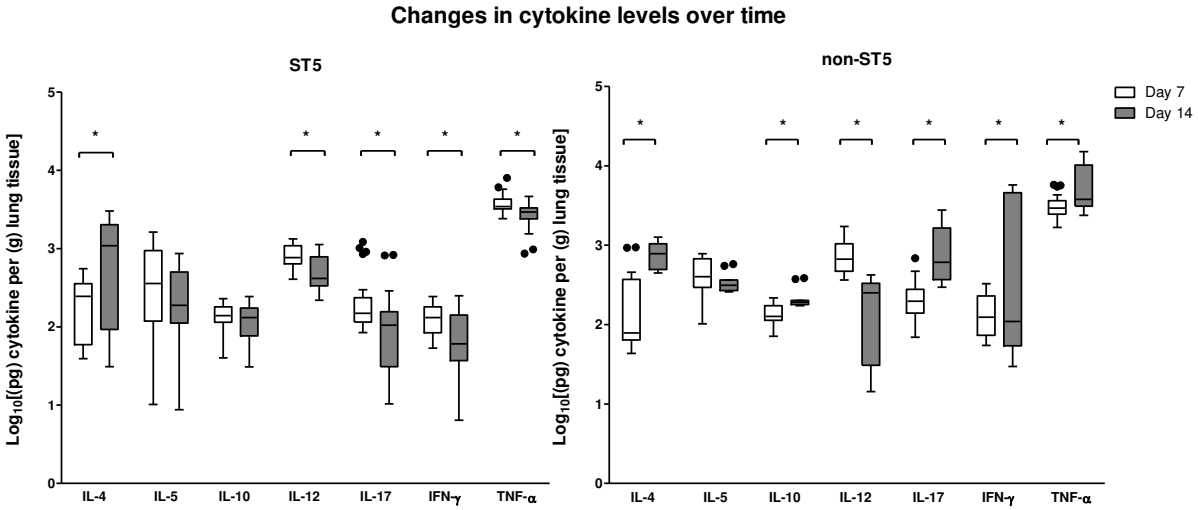

FIGURE 5: Genotype-specific changes of cytokine concentration from lung homogenate of A/J mice infected with 5x10^4 *C. neoformans* cells/mouse between day 7 and day 14 post-infection. Box and whisker plots compare levels of each cytokine between day 7 and day 14 for each genotype. The horizontal line within the box indicates the median, boundaries of the box indicate the 25th and 75th percentile and the whiskers indicate the highest and lowest values of the results; outliers are denoted as black dots. Data are standardized as picogram of cytokine per gram lung tissue. Asterisks show statistical significance by Mann-Whitney test.

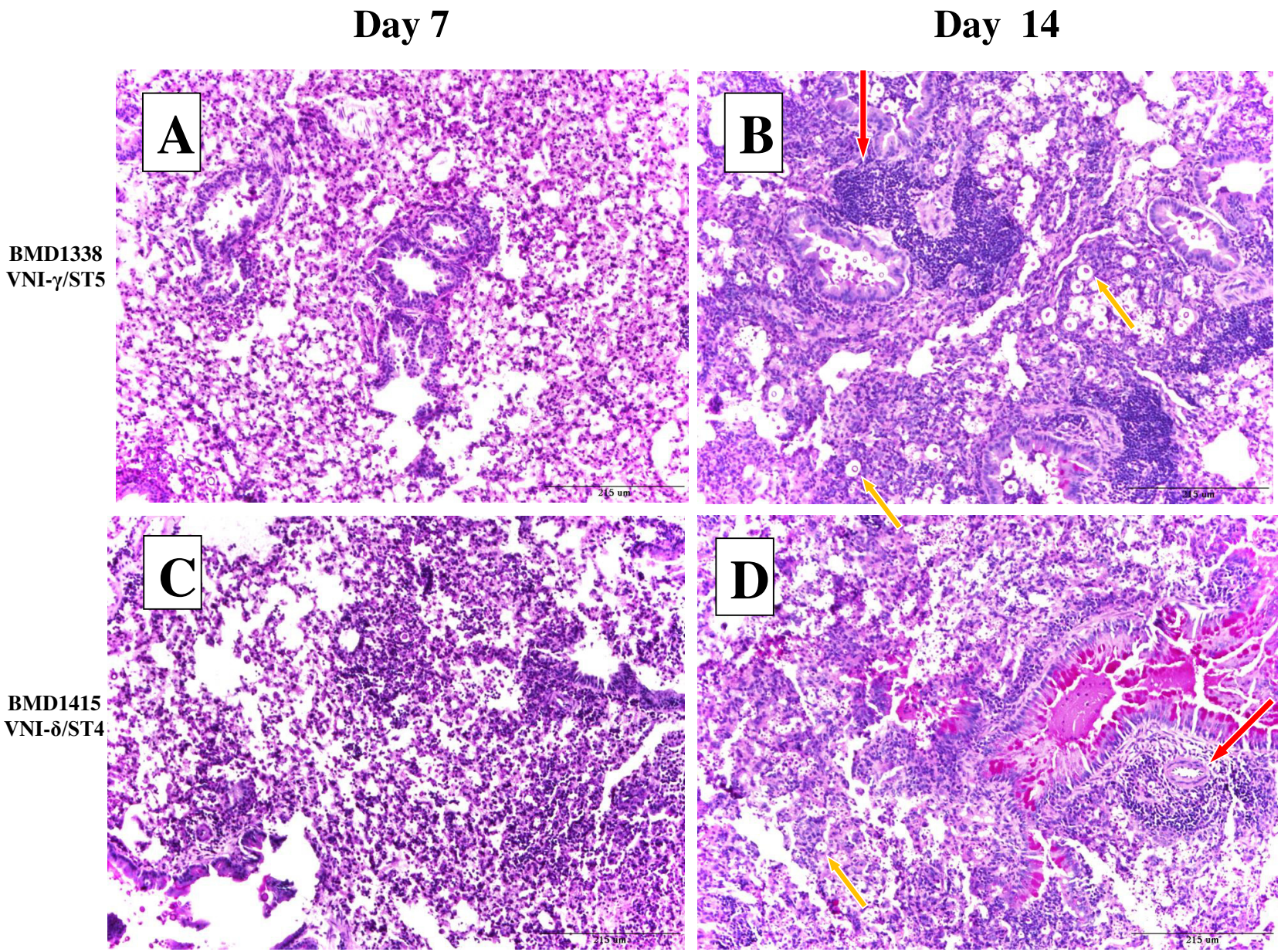
Day 7
Day 14
A
B
C
D
BMD1338
VNI-γ/ST5
BMD1415
VNI-δ/ST4
215 um
215 um
215 um
215 um

FIGURE 6: Periodic Acid Schiff (PAS) staining of pulmonary tissue from mice infected with BMD1338 and BMD1415 on days 7 ad 14. The two strains represent ST5 and non-ST5, respectively. A/J mice were inoculated intranasally with $5x10^4$ yeast cells. Lung specimens were harvested at days 7 and 14 for histopathological examination. Photomicrographs were obtained at 200X magnification; the scale bar represents 215 µm). (A-B): lung sections from mice infected with BMD1338 (VNI-γ/ST5) at day 7 and day 14, respectively. (C-D): lung sections from mice infected with BMD1415 (VNI-δ/ST4) at day 7 and day 14, respectively. Perivascular infiltration (red arrows) and necrosis are more marked by day 14 for both strains. Encapsulated yeasts (yellow arrows), notable for the larger cell size and capsule thickness of BMD 1338 compared with BMD1415.

TABLE 1 Strain source and typing (n=30)

Isolate data				Patient data	
Order	**Strain name**	**AFLP**	**MLST**	**Underlying Disease**	**Sex**
1	BK14	VNI-δ	4	HIV	M
2	BK163	VNI-δ	4	HIV	M
4	BK225	VNI-δ	4	HIV	M
6	BK48	VNI-δ	4	HIV	M
7	BK59	VNI-δ	4	HIV	F
8	BK69	VNI-δ	4	HIV	M
9	BK74	VNI-δ	4	HIV	M
10	BK80*	VNI-δ	4	HIV	M
11	BK87	VNI-δ	4	HIV	M
12	BK88	VNI-δ	4	HIV	M
13	BK89	VNI-δ	4	HIV	M
15	BMD1415*	VNI-δ	4	Lupus	M
3	BK218	VNI-δ	6	HIV	M
5	BK234	VNI-δ	6	HIV	F
14	BMD1367*	VNI-δ	306	Gastric cancer	F
16	BK147*	VNI-γ	5	HIV	M
17	BK44*	VNI-γ	5	HIV	M
18	BMD101	VNI-γ	5	None known	M
19	BMD1228	VNI-γ	5	None known	F
20	BMD1291	VNI-γ	5	None known	F
21	BMD1338*	VNI-γ	5	None known	M
22	BMD1353	VNI-γ	5	None known	M
23	BMD1452	VNI-γ	5	None known	F
24	BMD1646	VNI-γ	5	None known	M
25	BMD1716	VNI-γ	5	None known	F
26	BMD367	VNI-γ	5	None known	M
27	BMD673	VNI-γ	5	None known	F
28	BMD700*	VNI-γ	5	None known	M
29	BMD854	VNI-γ	5	None known	F
30	BMD899	VNI-γ	5	None known	F

AFLP = amplified fragment length polymorphism
MLST = multi locus sequence typing
M = Male, F = Female
** indicates isolates selected for mouse experiment*

TABLE 2 Variability in *in vitro* capsule thickness and cell diameter between ST5 and non-ST5 *Cryptococcus neoformans* strains from Vietnam

	MLST Group	
Variable	**ST5**	**Non-ST5**
Capsule Thickness (µm)		
Mean*	2.64	2.01
95% CI	2.49 - 2.79	1.94 - 2.07
Range	0.01 - 9.56	0.02 - 6.16
Coefficient of Variation$ (%)	0.63	0.37
Cell diameter (µm)		
Mean*	11.38	9.69
95% CI of Mean	10.96 - 11.79	9.52 - 9.87
Range	4.74 - 27.22	5.25 - 19.89
Coefficient of Variation$ (%)	0.41	0.20

** P<0.0001, t-test with Welch's correction.*

$ P< 0.0001, Fligner-Killeen test of homogeneity of variance.

TABLE 3 Tissue fungal burden in mice at days 7, 14 and death by infecting Sequence Type, log10Colony Forming Units of yeast per gram of tissue

	Fungal burden (Mean $\log_{10}$ colony forming units per gram of tissue) [95%CI]		
Tissue	**ST5**	**Non-ST5**	**P Value**
Lung (Day 7)	4.96 [3.86 - 6.05]	7.07 [6.85 - 7.29]*	<0.01
Brain (Day 7)	0.81 [0.38 - 1.24]	1.59 [0.87 - 2.30]	0.05
Lung (Day 14)	5.48 [4.34 - 6.62]	8.00 [7.77 - 8.23]*	<0.0001
Brain (Day 14)	1.56 [0.81 - 2.31]	1.91 [1.12 - 2.69]	0.36
Lung (Death)	3.81 [3.05 - 4.57]	6.53 [6.30 - 6.76]*	<0.0001
Brain (Death)	2.90 [2.23 - 3.56]	4.29 [3.90 - 4.68]*	0.01

**Mann-Whitney test.*

TABLE 4: Cytokine concentrations from lung homogenate of infected mice at day 7 and day 14 post-infection according to infecting *Cryptococcus neoformans* AFLP group

Cytokine		Mean cytokine concentration (pg per gram of lung tissue) [95%CI]		*P Value (ST5 vs non-ST5)
		ST5	Non-ST5	
Day 7				
Th-1	IL-12	853.12 [750.50 - 955.80]	822.87 [608.90 - 1037.00]	0.30
	IFN-γ	136.02 [115.00 - 157.00]	150.59 [105.80 - 195.30]	0.97
	TNF-α	3933.71 [3486.00 - 4381.00]	3256.25 [2630.00 – 3882.00]	**0.01**
Th-2	IL-4	230.79 [162.80 - 298.80]	253.24 [11.60 - 349.90]	0.92
	IL-5	561.05 [369.00 - 753.10]	459.85 [344.40 - 575.40]	0.91
	IL-10	145.01 [128.20 - 161.80]	139.99 [119.30 - 160.70]	0.68
Th-17	IL-17	268.48 [155.90 – 381.00]	243.41 [165.60 - 321.20]	0.24
TNF-α/IL-10 ratio		27.13	23.26	N/A
Day 14				
Th-1	IL-12	547.84 [412.40 - 683.30]	213.72 [120.50 - 306.90]	**<0.01**
	IFN-γ	91.2 [57.25 - 125.20]	1760.67 [166.50 - 3355.00]	0.09
	TNF-α	2802.36 [2385.00 - 3220.00]	6378.76 [3374.00 - 9384.00]	**<0.01**
Th-2	IL-4	1154.72 [673.50 – 636.00]	800.35 [604.70 – 996.00]	0.60
	IL-5	294.6 [170.40 - 418.80]	347.55 [279.20 - 415.90]	0.15
	IL-10	132.76 [102.10 - 163.40]	220.15 [172.40 - 267.90]	**0.01**
Th-17	IL-17	175.75 [65.54 – 286.00]	1012.49 [459.20 – 1566.00]	**0.01**
TNF-α/IL-10 ratio		21.11	28.97	N/A

** Mann-Whitney test.*